Development 135, 2093-2103 (2008) doi:10.1242/dev.015990

Gli3 coordinates three-dimensional patterning and growth of the tectum and cerebellum by integrating Shh and Fgf8 signaling

Sandra Blaess, Daniel Stephen and Alexandra L. Joyner*

The coordination of anterior-posterior (AP) and dorsal-ventral (DV) patterning of the mesencephalon (mes) and rhombomere 1 (r1) is instrumental for the development of three distinct brain structures: the tectum and cerebellum dorsally and the tegmentum ventrally. Patterning of the mes/r1 is primarily mediated by signaling molecules secreted from two organizers: sonic hedgehog (Shh) from the floor plate (DV) and Fgf8 from the isthmus (AP). Gli3, a zinc-finger transcription factor in the Shh signaling pathway, has been implicated in regulating *Fgf8* expression and is therefore a potential candidate for coordinating the action of the two organizers. By inactivating mouse *Gli3* at successive embryonic time points in vivo, we uncovered the extent and the underlying mechanism of Gli3 function in the mes/r1. We demonstrate that before E9.0, *Gli3* is required for establishing a distinct posterior tectum, isthmus and cerebellum, but does not play a role in the development of the tegmentum. Between E9.0 and E11.0, *Gli3* continues to be required for isthmus and cerebellum development, but primarily for defining the cerebellar foliation pattern. We show that *Gli3* regulates patterning of the isthmus and cerebellar anlage by confining *Fgf8* expression to the isthmus, and attenuates growth of dorsal r1 (before E11.0) and the dorsal mes and isthmus (beyond E11.0) through regulation of cell proliferation and viability. In conclusion, our results show that *Gli3* is essential for the coordinated three-dimensional patterning and growth of the dorsal mes/r1.

KEY WORDS: Anterior-posterior patterning, Dorsal-ventral patterning, Isthmic organizer, Mid/hindbrain, Mouse

INTRODUCTION

A fundamental question in developmental neuroscience is how the simple mammalian neural tube is transformed into the complex and intricate structures that constitute the adult brain. Patterning of tissues in three dimensions requires precise coordination of a number of basic developmental processes including cell proliferation, specification and migration. An ideal system in which to study patterning events is the brain region consisting of the mesencephalon (mes) and rhombomere 1 (r1). The mes and r1 are the primordia for the tectum [superior colliculus (SC) and inferior colliculus (IC)] and cerebellum dorsally, respectively, and for the tegmentum ventrally. Organizing centers that govern mes/r1 growth and patterning along the dorsal-ventral (DV) and anterior-posterior (AP) axes have been identified. AP patterning of the mes/r1 is mediated by fibroblast growth factor 8 (Fgf8), which is secreted by the isthmic organizer located at the mes/r1 boundary (Wurst and Bally-Cuif, 2001; Zervas et al., 2005). Sonic hedgehog (Shh), expressed in the notochord and the ventral midline (floor plate) of the neural tube, controls specification of ventral cell types in the tegmentum and formation of normal dorsal structures, as well as cell proliferation and survival (Agarwala et al., 2001; Bayly et al., 2007; Blaess et al., 2006; Corrales et al., 2006; Fedtsova and Turner, 2001; Ishibashi and McMahon, 2002). It remains to be addressed how these two signaling centers are integrated to control growth and patterning in three dimensions.

The zinc-finger transcription factor Gli3 influences multiple signaling pathways in the mes/r1. Gli3 is an essential downstream component of the Shh signaling pathway, and an increase in Gli3 repressor (Gli3R) levels is the primary cause of the dorsal mes/r1 defects in Shh signaling mutants (Blaess et al., 2006). Furthermore, Gli3 plays a role in regulating the *Fgf8* expression domain at the mes/r1 boundary (Aoto et al., 2002). Therefore, Gli3 could play a key role in coordinating three-dimensional patterning of the mes/r1 by affecting these two signaling pathways.

Only one mutation in mouse that is thought to represent a *Gli3*-null allele has been characterized. The lethal *Gli3 extratoe* (*Xt*) mutation causes multiple defects, including a background-dependent occurrence of exencephaly (Hui and Joyner, 1993; Maynard et al., 2002). In non-exencephalic embryos, however, tectum- and cerebellum-like structures develop, but are morphologically highly abnormal (Aoto et al., 2002; Blaess et al., 2006). The analysis of $Gli3^{Xt/Xt}$ mutants has so far provided little insight into Gli3 function in the mes/r1 and it remains unclear whether the defects result from changes in the expression of key DV patterning genes, abnormal growth and/or changes in Fgf8 signaling in the isthmic organizer (Aoto et al., 2002).

Gli3 transcription and protein activity are regulated at many levels by Shh signaling. In the absence of Shh activity, Gli3 is processed into an N-terminal repressor form that suppresses Shh target genes (Hu et al., 2006; Wang et al., 2000). Shh signaling attenuates the level of Gli3R, and full-length Gli3 can act as a weak activator (Gli3A) when the concentration of Shh is high (Bai et al., 2004; Dai et al., 1999; Wang et al., 2007). Gli3, however, is also transcriptionally downregulated in cells receiving high levels of Shh. Consequently, *Gli3* expression, which is initially found throughout the neural plate, is restricted to the intermediate and dorsal neural tube after E8.5 (Bai et al., 2002; Blaess et al., 2006; Hui et al., 1994; Marigo et al., 1996).

Activation of Shh target genes is primarily mediated by Gli1 and Gli2 (Fuccillo et al., 2006; Jacob and Briscoe, 2003). Gli2 requires Shh signaling to act as an activator (Gli2A), whereas Gli1 is a

Developmental Biology Program, Memorial Sloan-Kettering Cancer Center, 1275 York Avenue, Box 511, New York, NY 10021, USA.

*Author for correspondence (e-mail: joynera@mskcc.org)

Accepted 16 April 2008

transcriptional target of Gli2/3A and is itself a constitutive activator (Fuccillo et al., 2006; Jacob and Briscoe, 2003). We recently showed that Gli2A-mediated Shh signaling is the key regulator of the initial specification of ventral neurons in the embryonic mes/r1 before E11, and of granule cell precursor proliferation in the postnatal cerebellum (Blaess et al., 2006; Corrales et al., 2006; Corrales et al., 2004). It is unclear, however, whether Gli3A is also required for the development of these two regions.

Analysis of the severely abnormal *Gli3*$^{Xt/Xt}$ null mutants can only provide insight into the first crucial early developmental function of Gli3. To study the underlying mechanisms of Gli3 function we combined the analysis of null and time-specific conditional mutants by generating a *Gli3* conditional allele and inactivating *Gli3* in the mes/r1 at either E9.0 or E11.5. We demonstrate that *Gli3* is required to pattern dorsal mes/r1 into distinct structures before E9.0, continues to regulate the growth of the tectum and the cerebellum as well as cerebellar foliation between E9.0 and E11.0, and plays a role beyond E11.0 in regulating growth of the isthmus, SC and IC. We further show that the role of Gli3 in isthmic and cerebellar development, but not tectal patterning, is largely mediated through the repression of *Fgf8* expression in r1.

MATERIALS AND METHODS

Generation of *Gli3* conditional mutants

A 5.8 kb *Pst*I-*Mfe*I genomic fragment of *Gli3* containing intron 8 was inserted into a targeting vector upstream of a *neo* cassette flanked with Frt sites, with one loxP site 3′ to the *neo* cassette and a thymidine kinase (*TK*) cassette. Another loxP site containing an *Eco*RV site was inserted into a *Nhe*I site within intron 9 in a 4.8 kb *Mfe*I-*Kpn*I genomic fragment of *Gli3*. This fragment was inserted 3′ to the loxP site in the *neo-TK* vector.

Three targeted W4 (Auerbach et al., 2000) ES cell clones were identified (Matise et al., 2000) by Southern blot analysis using *Sph*I and a 1 kb external probe 3′ of the *Sph*I site, or using *Kpn*I and an internal probe containing *neo*. ES cell chimeras were generated through injection of C57BL/6 blastocysts (Skirball Transgenic Facility) (Papaioannou and Johnson, 2000). Chimeras were bred to C57BL/6 mice and heterozygous *Gli3*$^{flox\text{-}neo/+}$ offspring to SV129 *ACTB-Flpe* mice (Rodriguez et al., 2000) to produce *Gli3*$^{flox/+}$ heterozygotes lacking *neo*. *Gli3*$^{rec/+}$ mice carrying a loxP-mediated deletion were intercrossed or crossed with *Gli3*$^{Xt/+}$ mice (Hui and Joyner, 1993). Both *Gli3*$^{rec/rec}$ and *Gli3*$^{rec/Xt}$ E18.5 embryos displayed the same brain and limb phenotypes described in *Gli3*$^{Xt/Xt}$ embryos (see Fig. S1D-F in the supplementary material) (Hui and Joyner, 1993). Other phenotypes observed in *Gli3*$^{Xt/Xt}$ embryos, such as lethality at birth and exencephaly in some mutants, were also observed (data not shown). The *Gli3*^{flox} allele was genotyped using the following primers: S1, 5′-CTGGATGAACCAAG-CTTTCCATC-3′ and AS3, 5′-CTGCTCAGTGCTCTGGGCTCC-3′. For detecting the recombined allele, primers were S1 (as above) and AS2, 5′-CAGTAGTAGCCTGGTTACAG-3′.

Other alleles were genotyped as described: *Cre*, *Smo*^{flox}, *Smo*^{rec} (Blaess et al., 2006), *Fgf8* null (Chi et al., 2003) and *Gli3*^{Xt} null (Maynard et al., 2002). *Gli3*$^{Xt/+}$ mice were maintained on a C57/BL6 background; all other mouse lines were maintained on an outbred Swiss Webster background. Noon of the day a vaginal plug was observed was designated as E0.5; the day of birth was designated as P0.

Histology, immunohistochemistry and RNA in situ hybridization

Embryos/brains were fixed in 4% paraformaldehyde (PFA) at 4°C, processed for paraffin- or cryosectioning and sectioned at 7-12 μm. Antibody staining, BrdU labeling and RNA in situ hybridization were performed using standard methods. Primary antibodies: rabbit anti-TH (Chemicon, 1:500); rabbit anti-Ki67 (NovoCastra, 1:500); mouse anti-BrdU (BD-Bioscience, 1:100); rabbit anti- phosphohistone H3 (PH3) (1:500, Cell Signaling Technology); rabbit anti-caspase 3 (Cell Signaling Technology, 1:200); mouse anti-calbindin (Sigma, 1:1000); rabbit anti-calbindin (Swant, 1:5000); rabbit anti-Pax2 (Zymed, 1:500); rabbit anti-neurogranin (Chemicon, 1:500); mouse anti-Nkx6.1 [(Pedersen et al., 2006) Developmental Studies Hybridoma Bank, 1:100]. Apoptosis was quantified by immunostaining for cleaved caspase 3. Proliferation and/or cell cycle exit was quantified by PH3 immunostaining or BrdU pulse labeling (1 hour or 24 hours) followed by BrdU, BrdU/Ki67 immunostaining. Coronal sections of wild-type and conditional mutants (⩾3 embryos for each genotype and stage) were used. In situ hybridization and/or immunostaining for region-specific markers (En1 for mes/r1 at E9.5; Otx2 for mes; Pax7 for dorsal mes/r1; Pax6 for diencephalon) was performed on adjacent sections. Cells were counted in the ventral and dorsal mes and r1 (⩾3 sections) at E9.5 and E10.5 and either normalized for ventricle length (cleaved caspase 3, PH3) or total cell number (BrdU). At E12.5, cells in the dorsal mes (⩾3 sections) and in r1 and ventral mes (1-3 sections) were counted and normalized for ventricle length (PH3) or cell number (BrdU$^+$, Ki67$^+$/BrdU$^+$). Cell counts were performed using ImageJ.

Detailed protocols are available at http://www.mskcc.org/mskcc/html/77387.cfm.

RESULTS

Distinct temporal contributions of *Gli3* to growth and patterning of the midbrain and cerebellum

To study Gli3 function, we generated mice carrying a conditional *Gli3* mutant allele, *Gli3*^{flox}, in which two loxP sites flank exon 8 (see Fig. S1 in the supplementary material). Deletion of exon 8 and splicing from exon 7 to 9 result in a frameshift mutation upstream of the DNA-binding domain (*Gli3*^{rec}). Since we previously showed that a short period of gene function can be sufficient to rescue the most severe defects observed in null mutants (Blaess et al., 2006; Sgaier et al., 2007), *En1-Cre* was used to remove *Gli3* specifically in the mes/r1 by E9.0, about 36 hours after the onset of *Gli3* expression (Hui et al., 1994; Kimmel et al., 2000; Li et al., 2002). To assess whether Gli3 is required for mes/r1 development after midgestation, *Nestin-Cre* was used to remove *Gli3* from the entire neural tube around E11.5 (Blaess et al., 2006; Graus-Porta et al., 2001; Tronche et al., 1999). Indeed, inactivation of *Gli3* by E9 (*Gli3*$^{flox/Xt}$*;En1-Cre* mice, referred to as *En1-Gli3* cko) or E11.5 (*Gli3*$^{flox/Xt}$*;Nestin-Cre* mice, referred to as *Nes-Gli3* cko) resulted in rescue of the early postnatal lethality of *Gli3*-null mutants and the conditional knockout mice survived for several months.

The *Gli3* conditional mutants were first compared with *Gli3*-null mutants at E18.5, as the latter die at birth. *Gli3*-null mutants (*Gli3*$^{Xt/Xt}$, *Gli3*$^{Xt/rec}$ or *Gli3*$^{rec/rec}$) showed a phenotype of a variable nature in the midbrain and cerebellum at E18.5 (see Fig. S2A-J in the supplementary material), but the variability was independent of the allele (*rec* or *Xt*). Therefore, all three genotypes were used to represent the *Gli3*-null (*Gli3*$^{-/-}$) mutant phenotype. At the gross morphological level, the phenotype of E18.5 *Gli3*$^{-/-}$ mutants included: (1) a poorly foliated cerebellum that was not clearly separated from the isthmus; (2) an expanded isthmus-like region with ectopic cell clusters; (3) an overgrown tectum; (4) loss of the distinct morphology that normally defines the isthmus, IC and SC (8/11) (Fig. 1A,B,E,F; see Fig. S2A-J in the supplementary material). By contrast, the tegmentum of *Gli3*$^{-/-}$ mutants was morphologically unaffected and the size of the ventral nuclei comprising tyrosine hydroxylase (TH)-positive dopaminergic neurons or Isl1-positive motoneurons appeared similar to that of wild-type (WT) mice (Fig. 1I,J and data not shown).

Similar to *Gli3*$^{-/-}$ mutants, E18.5 *En1-Gli3* cko mutants had a normal tegmentum, and a misshapen and enlarged tectum and isthmus (Fig. 1C,G,K; see Fig. S2K,L in the supplementary material). In contrast to *Gli3*$^{-/-}$ mutants, however, the isthmus, IC and SC each appeared as morphologically distinct structures in the

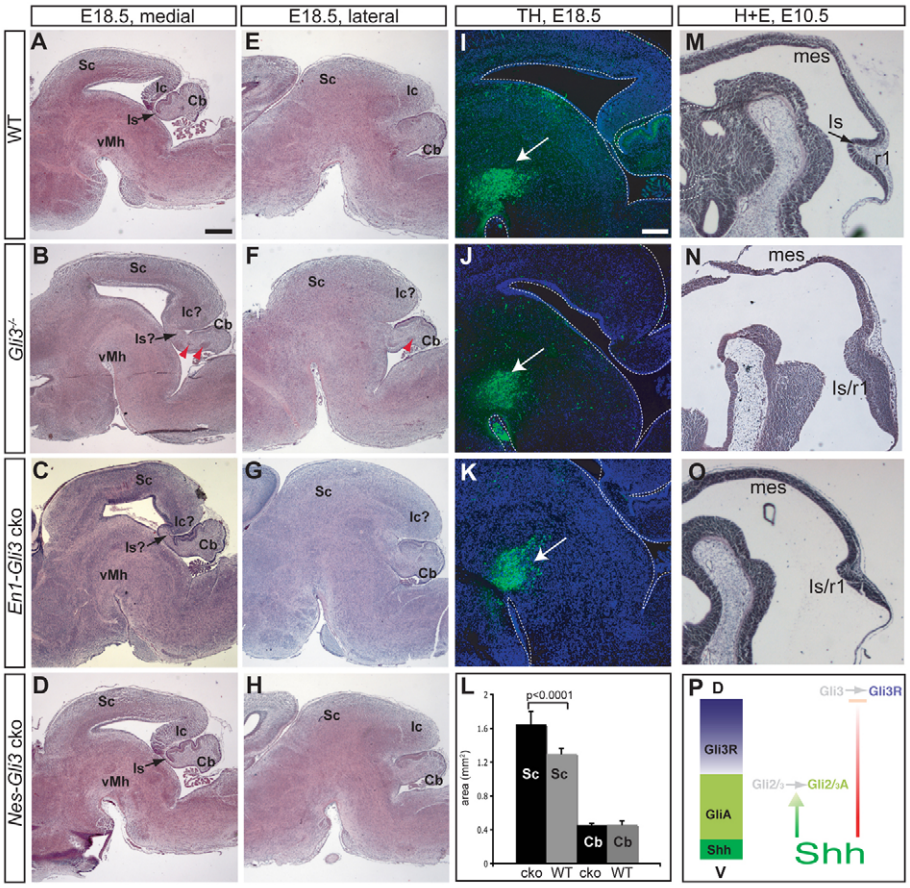

Fig. 1. Distinct temporal roles of *Gli3* in regulating midbrain and cerebellum development in mouse. (**A-H**) Hematoxylin and Eosin (H+E) staining of midline (A-D) and lateral (E-H) E18.5 sagittal brain sections. (B,F) In *Gli3*$^{-/-}$ mutants, the dorsal midbrain is enlarged and the distinct morphology of the inferior colliculus (Ic) and superior colliculus (Sc) is lost. Similarly, the isthmus (Is) and cerebellum (Cb) are not clearly separated and contain cell clusters (red arrowheads). The Cb is not foliated. The morphology of the ventral mid/hindbrain (vMh) appears normal. (C,G) In *En1-Gli3* cko mutants, the Sc, Ic, Is and Cb (arrow) are enlarged, and tectum, Is and Cb are morphologically distinct from one another. The Cb foliation pattern is abnormal. (D,H) In *Nes-Gli3* cko mutants, the Sc, Ic, Is and Cb are morphologically distinct, but the Sc, Ic and Is are increased in size. (**I-K**) Immunohistochemistry for tyrosine hydroxylase (TH) shows no change in dopaminergic neurons (green, arrows) in the mutants. DAPI staining is in blue. (**L**) Quantitative assessment of Cb and Sc size in wild-type (WT) and *Nes-Gli3* cko brains as means of samples from three different animals ±s.e.m. Student's *t*-test was performed. (**M-O**) H+E staining of E10.5 sagittal embryo sections. Note the increased size of the ventricle and increased thickness and abnormal morphology of the Is/r1 region in *Gli3*$^{-/-}$ and *En1-Gli3* cko mutants. (**P**) On the left is a schematic of Shh and Gli expression in the ventral (V) and dorsal (D) embryonic mes/r1. On the right, Shh signaling in the ventral and dorsal mes/r1: high levels of Shh induce Gli activator (GliA2/3, green) and inhibit (red) the formation of Gli3 repressor (Gli3R, purple) ventrally. Low levels of Shh decrease the formation of Gli3R dorsally. Gradients indicate high to low levels of expression/signaling. Scale bars: 500 μm in A-H; 250 μm in I-K,M-O.

majority of *En1-Gli3* cko mutants (9/16). Furthermore, the cerebellum was well developed, appeared to have a normal cytoarchitecture and had begun to foliate, although the foliation pattern was abnormal (Fig. 1C,G; Fig. 3O-Q; see Fig. S2K,L in the supplementary material). When *Gli3* function was left intact until E11.5 (*Nes-Gli3* cko mutants), all the morphological defects in the cerebellum, isthmus and tectum were rescued at E18.5 (Fig. 1A,D,E,H), but the size of the isthmus and of the entire tectum was significantly increased (Fig. 1A,D,E,H,L; see Fig. S2M,N in the supplementary material).

In summary, histological analysis indicates that *Gli3* is required for the dorsal mes/r1 primordium to form distinct brain structures before E9.0, and to establish the cerebellar foliation pattern and the normal size and shape of the isthmus and tectum between E9 and E11. Furthermore, *Gli3* regulates growth of the tectum and isthmus beyond E11.5.

Gli3 is required to regulate mes and r1 growth

To assess when the mes/r1 phenotypes arise in *Gli3* mutants, we analyzed E10.5 (*Gli3*$^{-/-}$ and *En1-Gli3* cko) and E12.5 (all mutants) embryos. We observed severe morphological defects in the mes/r1 of *Gli3*$^{-/-}$ and *En1-Gli3* cko mutant embryos, which in general were more pronounced in *Gli3*$^{-/-}$ mutants (Fig. 1M-O and data not shown): (1) the mesencephalic ventricle was expanded; (2) dorsal posterior mes, isthmus and r1 were not morphologically distinct from each other and the isthmic flexure was less prominent; (3) the thickness of the ventricular zone of the posterior dorsal mes, isthmus and r1 region was increased.

The increased growth of the mes/r1 in *Gli3* mutant embryos could be caused by a decrease in cell death or an increase in proliferation. A previous whole-mount analysis suggested that cell death is decreased in the mes/r1 at E8.5 and in the mes dorsal midline at E9.5 in *Gli3*$^{-/-}$ mutants (Aoto et al., 2002). To investigate whether decreased cell death could underlie the expansion of dorsal mes/r1 in *Gli3* mutant embryos, we analyzed the number of cleaved caspase-3-positive cells in the mes/r1 of E9.5 and E10.5 *En1-Gli3* cko mutants. There was a trend toward decreased cell death in *En1-Gli3* cko mutants as compared with WT, but only in the E10.5 dorsal mes/r1 (see Fig. S3D,E in the supplementary material). However, because these results indicate that cell death is not dramatically reduced in the absence of *Gli3*, reduced cell death is unlikely to be the sole cause of mes/r1 overgrowth in the mutants.

To address whether increased proliferation contributes to the increase in mes/r1 size, we analyzed ventral and dorsal mes/r1 of WT and cko mutant embryos for BrdU incorporation (1-hour pulse, S phase of the cell cycle) or for expression of phosphohistone H3 (PH3) (G2–M phase of the cell cycle). Quantitative assessment of proliferating cells indicated a slight increase in proliferation in the dorsal mes/r1 of *En1-Gli3* cko mutants at E9.5 and E10.5 and in the dorsal mes of E12.5 *Nes-Gli3* cko mutants as compared with WT

(see Fig. S3A-C in the supplementary material). Importantly, in the ventral mes/r1, proliferation appeared to be similar in cko mutants and WT, consistent with the lack of a ventral phenotype at E18.5. Since an increased proliferation rate could be caused by a shortening of cell cycle length or by a delay in differentiation, we analyzed the cell cycle exit rate in E12.5 WT and *Nes-Gli3* cko mutants (Chenn and Walsh, 2002). We quantified the percentage of differentiating cells ($BrdU^+$ $Ki67^-$ cells/$BrdU^+$ cells) 24 hours after BrdU administration and did not observe an obvious changes between WT and mutant in ventral or dorsal mes or r1 (see Fig. S3F in the supplementary material). Thus, the increase in proliferation is not due to a decreased ability of cells to leave the cell cycle. In summary, these data demonstrate that *Gli3* is an important regulator of the growth of dorsal r1 (up to E11.0) and mes (beyond E11.0), modulating both cell proliferation (attenuation) and cell death (augmentation).

Gli3 is required for proper establishment of the inferior colliculus before E9.0

To investigate whether the abnormal tectal morphology in *Gli3* mutants is due to the observed mes overgrowth or to a direct requirement for *Gli3* in tectal patterning, we analyzed the expression of SC and IC markers at E18.5. We used *En1* as a marker for the IC because *En1* is normally expressed strongly throughout the IC and at lower levels in the posterior SC (Fig. 2A). *Otx2* was used as an SC marker because its expression in the superficial layers of the SC is clearly distinguishable from the *Otx2* expression in the IC ventricular zone (Fig. 2E). In $Gli3^{-/-}$ mutants, *En1* expression was very weak and was confined to the most posterior tectum (3/3), even in mutants in which the tectum appeared to be organized into an SC and IC at a morphological level (2/3) (Fig. 2B). In *En1-Gli3* cko mutants, *En1* expression was stronger and broader than in $Gli3^{-/-}$ mutants, but was restricted to a more posterior tectal region than in WT brain (3/3) (Fig. 2C). These data indicate that the IC was not properly specified in the mutants. This was also evident by *Otx2* expression, which was not restricted to the ventricular layer of the posterior tectum in $Gli3^{-/-}$ and *En1-Gli3* cko mutants. In addition, the thickness of the *Otx2*-positive layer was increased in the SC of $Gli3^{-/-}$ and *En1-Gli3* cko mutants, consistent with the tectal overgrowth in these mutants. As expected, given the normal tectal morphology of E18.5 *Nes-Gli3* cko mutants, the *En1* and *Otx2* expression domains were comparable to WT (Fig. 2A,E,D,H).

Despite the abnormal *En1* and *Otx2* expression in the posterior tectum, this region was not transformed into SC in the mutants, as the AP extent of the *Otx2* expression domain in the superficial layers of the SC in $Gli3^{-/-}$ and *En1-Gli3* cko mutants was comparable to WT (Fig. 2F,G). Furthermore, neurogranin, which is expressed in differentiated cells in the lateral IC at E18.5 and in the entire IC at P16 (Fig. 2I,L), was found to be expressed in the lateral tectum of E18.5 $Gli3^{-/-}$ mutants. The neurogranin expression domain, however, was severely reduced and shifted anteriorly (3/3) (Fig. 2J). In P16 *En1-Gli3* cko mutants, neurogranin immunostaining revealed a more elongated IC domain than in WT (Fig. 2L,M). By contrast, the shape of the IC in P16 *Nes-Gli3* cko mutants was comparable to WT, even though the size of the IC was increased (Fig. 2L,N). These data indicate that *Gli3* is required for proper establishment of the IC before E9.0, regulates normal IC morphology between E9.0 and E11.0 and growth beyond E11.0. By contrast, *Gli3* is not required for establishing the SC, although it plays a prolonged role in controlling normal SC growth.

Gli3 regulates proper establishment of the isthmus and cerebellum before E9.0 and cerebellar foliation between E9.0 and E11.0

To study the cellular phenotype of the isthmus-cerebellum-like region in $Gli3^{-/-}$ mutants, we analyzed markers for cerebellar and isthmic cell types. In the E18.5/P0 WT cerebellum, Purkinje cells are organized in a layer underlying Math1 (Atoh1)-positive granule cell precursors in the external granule cell layer (Fig. 3A,C,F,I). At this stage, all Purkinje cells express the retinoic acid receptor-related

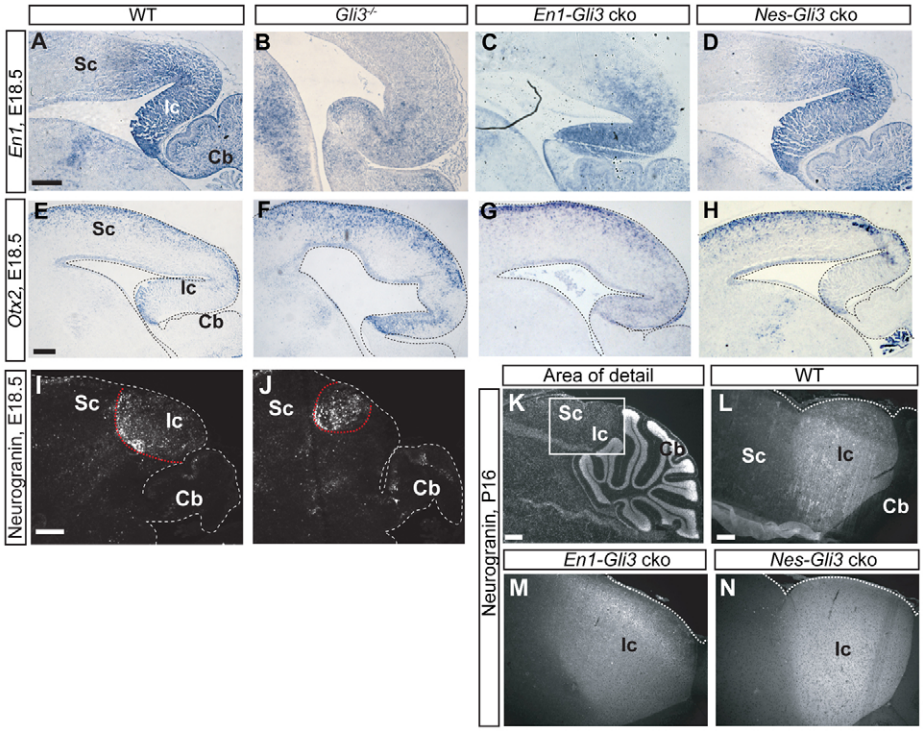

Fig. 2. *Gli3* is required for proper establishment of the inferior colliculus. (**A-D**) *En1* RNA expression in the E18.5 inferior colliculus (Ic) and posterior superior colliculus (Sc) in sagittal sections from WT mouse (A). *En1* expression is severely reduced in $Gli3^{-/-}$ mutants, slightly reduced in *En1-Gli3* cko and normal in *Nes-Gli3* cko mutants (B-D). (**E-H**) Expression of *Otx2* RNA in superficial layers of the Sc and in the ventricular layer of the Ic is comparable in WT (E) and *Nes-Gli3* cko brains (H). In $Gli3^{-/-}$ and *En1-Gli3* cko mutants, *Otx2* is expressed throughout the posterior tectum and the thickness of the *Otx2*-positive layer is increased in the Sc (F,G). (**I**,**J**) Immunohistochemistry for neurogranin on E18.5 sagittal sections. The neurogranin-positive domain (outlined in red) is reduced and shifted posteriorly in $Gli3^{-/-}$ mutants. (**K-N**) DAPI staining (K) and immunohistochemistry for neurogranin (L-N) at P16 show that the Ic is abnormally shaped in *En1-Gli3* cko, but not in *Nes-Gli3* cko mutants. Scale bars: 250 μm in A-H,I,J,L-N; 500 μm in K.

orphan receptor alpha (RORα), while a large subset expresses calbindin and inositol 1,4,5-trisphosphate receptor 1 (IP3R1; Itpr1 – Mouse Genome Informatics) (Fig. 3F,I and data not shown). Pax2 is expressed throughout the isthmus and deeper cerebellum where it marks (among other cell types) a subset of interneuron precursors (Fig. 3L) (Maricich and Herrup, 1999).

In *Gli3*$^{-/-}$ mutants, the cerebellar external granule cell layer did not extend into the anterior area of the medial isthmus-cerebellum-like region, suggesting that the anterior region might be transformed into isthmus (Fig. 1B; Fig. 3B,D). This anterior area, however, did not contain Pax2-positive cells, but instead had clusters of RORα- and IP3R1-positive Purkinje cells, indicating that this region had some characteristics of the cerebellum rather than of the isthmus (Fig. 3G,J,M and data not shown). The organization of the posterior isthmus-cerebellum-like region had some similarities to WT cerebellum, with a relatively normal distribution of Pax2-positive cells and RORα- and IP3R1-positive Purkinje cells underlying a Math1-positive external granule cell layer (Fig. 3B,D,G,J,M and data not shown). The Purkinje cell layer, however, was thicker than normal and did not consistently extend into the most posterior area. In addition, Purkinje cell axons that form bundles in WT were highly disorganized in *Gli3*$^{-/-}$ mutants (Fig. 3F,G and data not shown). This disorganization of Purkinje cells was equally severe in more-lateral regions of the cerebellum (data not shown). These results indicate that the anterior isthmic-cerebellar region is not properly specified in *Gli3*$^{-/-}$ mutants and the posterior isthmus-cerebellum area is not organized into a normal cerebellar cytoarchitecture.

In P0 *En1-Gli3* cko mutants, the defects in cerebellar cytoarchitecture were partially rescued, based on marker analysis (Fig. 3E,H,K,N and data not shown). Purkinje cell axons projected aberrantly into the posterior isthmus and some Purkinje cells formed clusters in the anterior isthmic region (Fig. 3H,K), suggesting that the isthmus-cerebellum boundary was not properly established in *En1-Gli3* cko mutants. Furthermore, at E18.5 and all the postnatal stages analyzed (P2, 5, 8, 16 and 30), the cerebellar foliation pattern was clearly abnormal and varied between mutants (Fig. 3O-Q; see Fig. S2K,L in the supplementary material). Interestingly, these defects in foliation were not associated with major changes in AP gene expression domains, as the expression of *Otx2* (posterior region) and of *Runx1* (central region) in the external granule cell layer were comparable to WT (data not shown). Consistent with the histological analysis, the cytoarchitecture, morphology and foliation

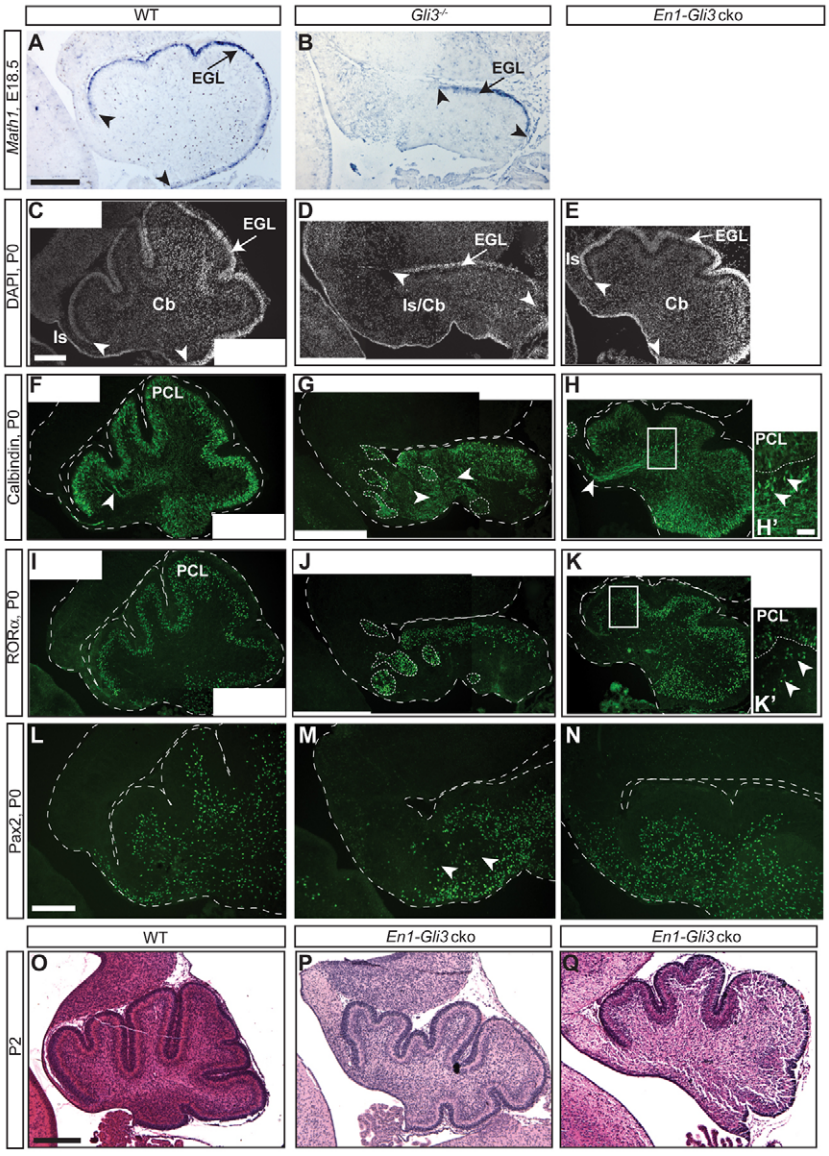

Fig. 3. *Gli3* regulates proper establishment of the isthmus and cerebellum. (**A-E**) RNA in situ hybridization for *Math1* and DAPI staining show that the external granule cell layer (EGL) is absent from the most posterior and anterior parts (arrowheads) of the isthmus-cerebellar like (Is/Cb) region in *Gli3*$^{-/-}$ mutants, but is comparable to WT in *En1-Gli3* cko mutants (arrowheads). (**F-N**) Immunohistochemistry on adjacent sections. (F-K) In the WT, Purkinje cells (PC) positive for calbindin and RORα (green) are organized in a several-cell-deep layer (PCL) underlying the EGL and project into the deeper Cb (arrowheads). In *Gli3*$^{-/-}$ mutants, only a rudimentary PCL forms with disorganized projections (arrowheads), and many PC remain in clusters in the deeper Is/Cb (outlined). (H,K) In *En1-Gli3* cko mutants, most PC are located within the PCL, with only some scattered PC in the underlying areas (H′,K′, arrowheads) and in ectopic clusters in the anterior Is (outlined). Some PC axons project into the Is (H, arrowhead). (L,M) Pax2 (green) is expressed in a scattered pattern throughout the Is and Cb (except the EGL and PCL) in WT and *En1-Gli3* cko mutants, but is not expressed in the anterior (EGL-free) region in *Gli3*$^{-/-}$ mutants and is excluded from the PC clusters (M, arrowheads). (**O-Q**) H+E staining of P2 sagittal sections shows the abnormal foliation pattern in *En1-Gli3* cko mutants. Brain regions are outlined where necessary. Note that some of the pictures presented are composites of two images (C,D,F,G,I,J). Scale bars: 200 μm in A-N; 20 μm in H′,K′; 500 μm in P-Q.

pattern of E18.5 and postnatal *Nes-Gli3* cko cerebella were similar to those of WT (Fig. 1A,D and data not shown). In conclusion, *Gli3* is required primarily before E9.0 for the proper specification of the isthmus and cerebellum, including the formation of normal cerebellar cytoarchitecture, and between E9.0 and E11.0 for establishing the stereotypic cerebellar foliation pattern.

Gli3R is not involved in attenuating GliA-mediated signaling in the dorsal mes/r1

Since Shh signaling induces ventral structures in the neural tube, one possible reason for the abnormal patterning of the IC, isthmus and cerebellum in *Gli3*$^{-/-}$ and *En1-Gli3* cko mutants is a Shh-induced ventralization of dorsal structures. To address this, we investigated whether the expression of ventrally (*Gli1*, *Nkx2.2* and *Nkx6.1*) and dorsally [*Pax7*, *Gbx2*, ephrin A5 (*Efna5*)] restricted genes is altered in the mes/r1 of *Gli3* mutants. Surprisingly, no dorsal expansion of *Gli1*, *Nkx2.2* or *Nkx6.1* was observed in *Gli3*$^{-/-}$ and *En1-Gli3* cko mutants (Fig. 4D-I and data not shown). Furthermore, in both *Gli3*$^{-/-}$ and *En1-Gli3* cko mutants, *Pax7* encompassed a similar dorsal domain as in WT embryos, indicating further that the dorsal mes/r1 was not ventralized in *Gli3* mutants (Fig. 4A-C). In addition, expression of *Gbx2* in dorsal r1 and of *Efna5* in dorsal-posterior mes were maintained in *Gli3*$^{-/-}$ and *En1-Gli3* cko mutant embryos (data not shown). In summary, these results show that *Gli3* does not play a major role in establishing DV spatial molecular patterning in the mes/r1.

The unaltered DV gene expression domains in *Gli3* mutants indicate that there is no ectopic GliA-mediated Shh signaling activity in the dorsal mes/r1 in the absence of *Gli3*. To definitively demonstrate that GliA-mediated Shh signaling does not contribute to the patterning and growth defects in *Gli3* mutants, we generated double cko mutants for *Smo* and *Gli3* (*En1-Gli3;Smo* cko), as removal of *Smo* results in the absence of GliA activity. Indeed, we found that E12.5 and P0 *En1-Gli3;Smo* cko mutant embryos had a tectal and isthmus phenotype very similar to that of *En1-Gli3* cko mutants (Fig. 4K-M; compare Fig. 4J with Fig. 1C). The morphology and overgrowth of r1 in *En1-Gli3;Smo* cko mutants was also similar to that shown by *En1-Gli3* cko mutants at E12.5. At P0, the overall size of the cerebellum and thickness of the external granule cell layer, however, were reduced (Fig. 4J and data not shown), resembling the *En1-Smo* cko phenotype that results from severely decreased granule cell precursor proliferation after E16.5 (Blaess et al., 2006; Corrales et al., 2006). This indicates that the overgrowth in the *En1-Gli3;Smo* cko cerebellar anlage is initially caused by loss of Gli3R (before E16.5), whereas after E16.5 the loss of Gli1/2A-mediated Shh signaling downstream of Smo results in reduced cerebellum growth owing to decreased granule cell precursor proliferation. In summary, these data demonstrate that the initial phenotypes in the dorsal mes/r1 of *Gli3* mutants result from a loss of Gli3R activity, rather than from ectopic GliA-mediated Shh signaling.

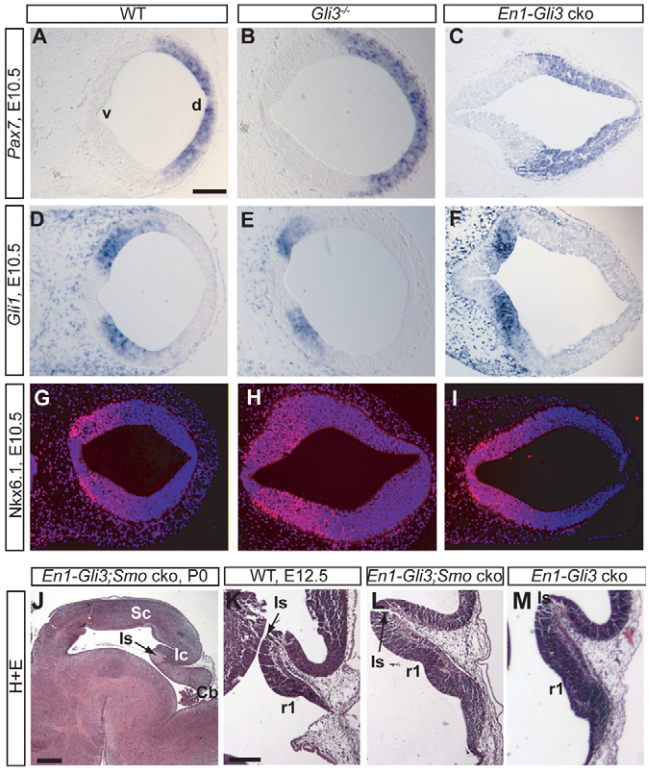

Fig. 4. *Gli3* is not required to establish DV gene expression domains or to inhibit activating Shh signaling. (**A-I**) RNA in situ hybridization for *Pax7* (A-C, dorsal marker) and *Gli1* (D-F, ventral marker) and immunohistochemistry for Nkx6.1 (G-I, ventral marker) on transverse sections of E10.5 mouse embryos show that expression of these genes in *Gli3*$^{-/-}$ and *En1-Gli3* cko mutants is comparable to WT. (**J-M**) H+E staining on P0 (J) and E12.5 (K-M) sagittal sections. The phenotypes of the Sc, lc and ls are comparable in P0 *En1-Gli3;Smo* cko and *En1-Gli3* cko mutants. Note that the Cb is small and unfoliated, with a thin external granule cell layer. (K-M) At E12.5, the size of r1 is increased in both *En1-Gli3* and *En1-Gli3;Smo* cko mutants as compared with WT. v, ventral; d, dorsal. Scale bars: 125 μm in A-I; 500 μm in J; 200 μm in K-M.

Gli3 is not required for roof plate induction in the mes/r1

Since defects in the roof plate contribute to the telencephalic phenotype in *Gli3*$^{-/-}$ mutants (Grove et al., 1998; Theil et al., 2002), we assessed whether alterations in signaling from the mes/r1 roof plate cause the dorsal mes/r1 phenotypes of *Gli3* mutants. The expression of two secreted factors involved in the organizing function of the roof plate, *Wnt1* and *Gdf7*, was maintained in the roof plate of *Gli3*$^{-/-}$ and *En1-Gli3* cko embryos at E9.5 and E10.5 (Fig. 5A-F and data not shown). In addition, *Msx1*, which is a downstream target of BMP signaling (Alder et al., 1999; Bei and Maas, 1998), was present in the roof plate in *Gli3*$^{-/-}$ and *En1-Gli3* cko mutants (Fig. 5G,H and data not shown). Finally, expression of *Axin2*, a target of Wnt signaling (Jho et al., 2002), was not grossly altered in E10.5 *Gli3*$^{-/-}$ or *En1-Gli3* cko mutant embryos (Fig. 5I,J and data not shown). In summary, *Gli3* does not appear to play a major role in establishing or maintaining the mes roof plate.

Gli3R is required to downregulate Fgf in dorsal r1

Since changes in DV patterning or roof plate signaling do not seem to account for the dorsal mes/r1 phenotype in *Gli3* mutants, we next examined whether alterations in the Fgf8 signaling pathway, which is a primary regulator of AP patterning, could contribute to the dorsal mes/r1 defects in *Gli3* mutants. Based on whole-mount analysis, it has been reported that *Fgf8* expression is expanded in E9.5 and E10.5 *Gli3*$^{-/-}$ mutants, whereas the *Fgf8* domain is reduced when Shh signaling is decreased and Gli3R is increased (Aoto et al., 2002; Blaess et al., 2006). We first analyzed *Fgf8* expression in spatial and temporal detail on sagittal sections of *Gli3* mutant embryos. Indeed, we observed ectopic *Fgf8* expression, but only in medial r1 in both

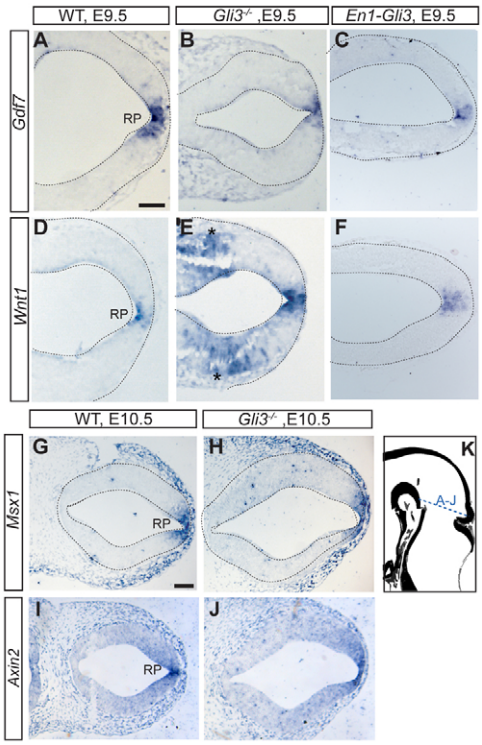

Fig. 5. *Gli3* is not required to establish the mes/r1 roof plate. (**A-F**) RNA in situ hybridization for *Gdf7* and *Wnt1* on transverse sections of E9.5 mouse embryos. *Gdf7* and *Wnt1* are expressed in the roof plate (RP) in the WT and mutant embryos. Note that the *Wnt1*-positive domain in the lateral mes (*) is in the isthmic region. (**G-J**) RNA in situ hybridization for *Msx1* and *Axin2* on E10.5 transverse sections shows that RP expression is not changed in $Gli3^{-/-}$ mutants. (**K**) Plane of section is indicated in this schematic. The neural tube is outlined where necessary. Scale bars: 100 μm.

E9.5 and E10.5 $Gli3^{-/-}$ (Fig. 6G-I and data not shown) and *En1-Gli3* cko (data not shown) mutants. By E12.5, shortly before the normal termination of *Fgf8* expression, ectopic *Fgf8* expression was restricted to the posterior-most part of medial r1 in $Gli3^{-/-}$ (data not shown) and *En1-Gli3* cko (Fig. 6J,K) mutants. Interestingly, this region corresponds to the rhombic lip in the WT and normally expresses *Wnt1* and *Math1* (Fig. 6A,B,D,E and data not shown). Furthermore, *Fgf17*, which also plays a role in AP patterning of the mes/r1 and is expressed in a broader domain than *Fgf8* in the WT (Xu et al., 2000), and sprouty 1 (*Spry1*), a direct target of Fgf8 signaling (Liu et al., 2003), were expanded posteriorly in both *Gli3* mutants, but were not altered in the mes (Fig. 6M-Q,S-W). To address whether Gli3R rather than Shh signaling is required for *Fgf8* suppression in r1, we analyzed E12.5 *En1-Gli3;Smo* cko mutants and found that similar to *En1-Gli3* cko mutants, *Fgf8*, *Fgf17* and *Spry1* were expressed ectopically in dorsal-posterior r1 (data not shown).

Consistent with the normal tectal and cerebellar morphology in *Nes-Gli3* cko mutants, no changes in *Fgf8*, *Fgf17* or *Spry1* expression were observed in these mutants at E12.5 (Fig. 6F,L,R,X). In addition, in all *Gli3* mutants the expression domains of *Wnt1* and *Otx2* in the mes appeared normal (anterior to *Fgf8* expression) and *Gbx2* expression in r1 was maintained (Fig. 6A-F and data not shown). These results indicate that changes in gene expression are specific to the Fgf pathway and that the boundary between the mes and r1 is intact in *Gli3* mutants. Thus, Gli3R is required to inhibit *Fgf8* and *Fgf17* expression beyond E9.0, but only in dorsal-medial r1.

Gli3 mediates isthmic and cerebellar patterning through regulation of Fgf8 expression

To test whether the expansion of Fgf expression in r1 is responsible for any of the dorsal defects in *Gli3* mutants, we removed one copy of *Fgf8* in $Gli3^{-/-}$ mutants. Histological analysis of $Gli3^{-/-};Fgf8^{+/-}$ mutants (n=4) at E18.5 or P0 showed a striking partial rescue of the defects seen in the isthmus-cerebellum-like region, but not tectum, of $Gli3^{-/-}$ mutants (Fig. 7; see Fig. S4 in the supplementary material). Unlike any of the $Gli3^{-/-}$ littermates, the cerebellum of all $Gli3^{-/-};Fgf8^{+/-}$ mutants had begun to foliate at P0 and the external granule cell layer extended along the AP length of the medial cerebellum (Fig. 7A,E; for a direct comparison of littermates see Fig. S4A-H in the supplementary material). In addition, the isthmus appeared to have formed, based on morphology and the expression of Pax2 (Fig. 7A,H; see Fig. S4A-H in the supplementary material). Marker analysis further revealed a more normal organization of Purkinje cells, although cell clusters remained in and near the isthmus region, showing that a separation of isthmus and cerebellum was not fully established (Fig. 7F,G; see Fig. S4I,J in the supplementary material).

Although the isthmus-cerebellar phenotype was partially rescued in the $Gli3^{-/-};Fgf8^{+/-}$ mutants as compared with $Gli3^{-/-}$ single mutants, the tectal phenotype was similar to $Gli3^{-/-}$ single mutants. The tectum was enlarged, the IC was not clearly distinguishable and the range of morphological abnormalities was comparable to that of $Gli3^{-/-}$ mutants (Fig. 7A; Fig. 1B; see Fig. S2A,C,E,G,I and Fig. S4 in the supplementary material). Furthermore, *En1*, *Otx2* and neurogranin were abnormally expressed in the posterior tectum, similar to in $Gli3^{-/-}$ mutants (Fig. 7B-D; Fig. 2A,B,E,F). These findings provide genetic evidence that a major role of Gli3R in regulating the organization of cerebellar and isthmic cytoarchitecture is to localize *Fgf8* expression to dorsal-medial r1.

DISCUSSION

Distinct temporal functions of Gli3 in midbrain and cerebellum development

By studying the sequential cellular and genetic changes underlying *Gli3* function in mes/r1 development we demonstrate that Gli3R is a crucial regulator of growth and patterning of the dorsal mes/r1, whereas neither Gli3R nor Gli3A is required for development of the ventral mes/r1 (summarized in Fig. 8A). We show that dorsally, Gli3 has a prolonged role in attenuating the growth of r1 (before E11.0) and of the mes and isthmus (beyond E11.0) through reducing cell proliferation and promoting cell death. Importantly, analysis of *Gli3;Smo* double mutants demonstrates that normally it is Gli3R that attenuates growth in the mes/r1 and that factors other than Shh must stimulate mes/r1 proliferation. We further show that Gli3R has additional functions in patterning of the dorsal mes/r1. Before E9.0, Gli3R is required to establish a normal IC and a distinct isthmus and anterior cerebellum, as well as a normal cytoarchitecture. Between E9.0 and E11.0, Gli3R prevents Purkinje cells and their axons from entering the isthmus and is involved in setting up a normal foliation pattern. Finally, we demonstrate that the loss of the distinct separation between isthmus and cerebellum in *Gli3*-null mutants, as well as the abnormal cytoarchitecture in this region, are caused by ectopic expression of *Fgf8* in r1.

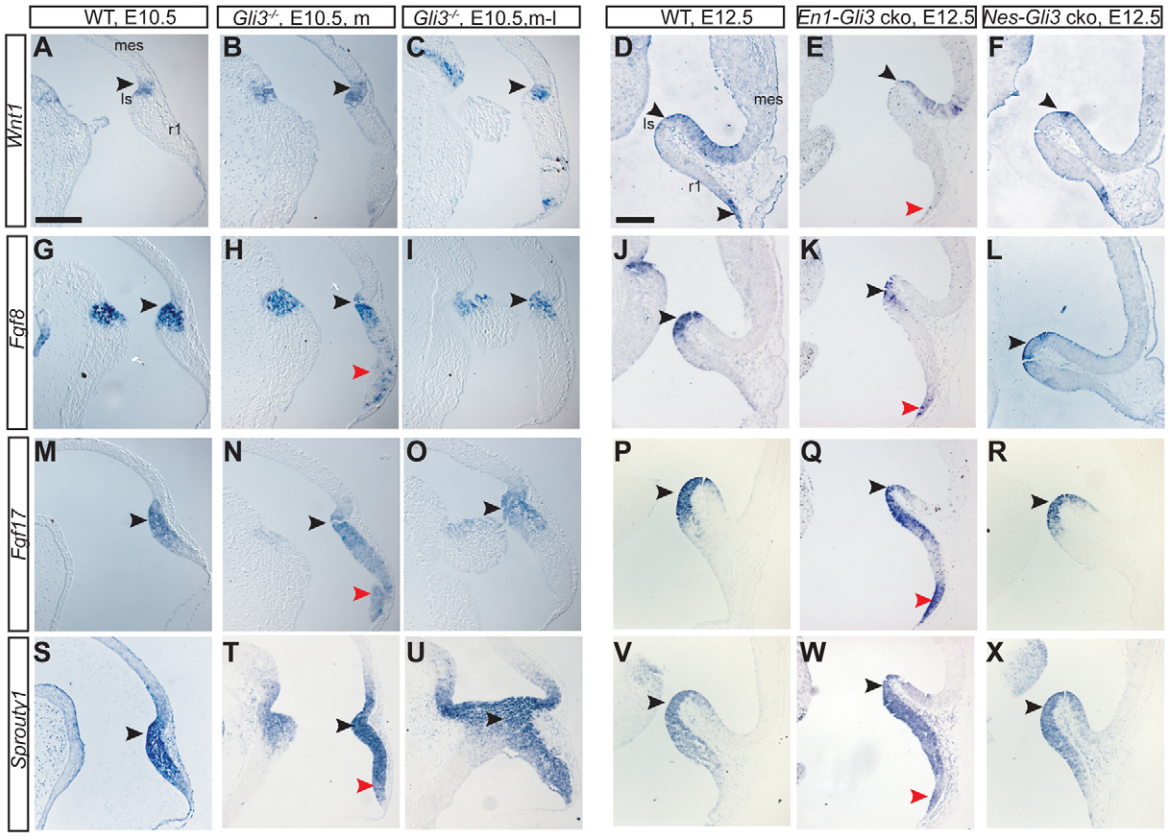

Fig. 6. *Gli3* is required to restrict Fgf expression to the isthmus. (**A-X**) *Wnt1, Fgf8, Fgf17* and *Spry1* RNA expression in mouse embryos at E10.5 and E12.5. Posterior mes, Is and r1 are shown (see Fig. 5K). Black arrowheads indicate normal expression, red arrowheads ectopic gene expression. (A-F) The *Wnt1* expression domain is unaltered in *Gli3* mutants. *Fgf8* (G-I), *Fgf17* (M-O), and *Spry1* (S-U) domains are expanded into medial, but not lateral, r1 in E10.5 $Gli3^{-/-}$ mutants. In E12.5 *En1-Gli3* cko mutants, ectopic expression of *Fgf8* (J,K), *Fgf17* (P,Q), and *Spry1* (V,W) is restricted to the most posterior region of medial r1, where *Wnt1* (D,E) is normally expressed. (L,R,X) *Fgf8*, *Fgf17* and *Spry1* expression is normal in *Nes-Gli3* cko mutants. Scale bars: 200 μm.

Gli3R is required to restrict *Fgf8* expression to the isthmus

We and others showed previously that *Fgf8* expression in the isthmic organizer is reduced when Gli3R is upregulated (*Shh/Smo* mutants) and increased when *Gli3* is absent ($Gli3^{-/-}$ mutants) (Aoto et al., 2002; Blaess et al., 2006). We built on these findings by showing that complete absence of *Gli3* as well as inactivation of *Gli3* at E9.0 (*En1-Gli3* cko mutants) result in an expanded expression domain of not only *Fgf8*, but also *Fgf17* and the Fgf8 downstream target *Spry1*. Furthermore, the expansion occurs only in the dorsal-medial region of r1 and, interestingly, this region includes the rhombic lip region. Moreover, the ectopic Fgf expression in r1 in the absence of *Gli3* is not diminished when Shh signaling is abolished (*En1-Gli3;Smo* cko mutants). Thus, Gli3R and not Shh activator signaling is required to restrict *Fgf8/Fgf17* expression to the isthmus. These results raise the question whether Gli3 might regulate *Fgf8* expression directly. Sequence analysis of the known *Fgf8* regulatory elements (Beermann et al., 2006), however, did not reveal any canonical Gli binding sites (Vokes et al., 2007) in these conserved regions (S.B. and J. Hastings, unpublished).

Fgf8 expression in the WT mes/r1 initially encompasses the isthmus and most of dorsal r1 at E8.5, and then becomes restricted to the isthmus by E10.5 (Crossley and Martin, 1995). Although there is evidence that the transcription factors *Otx2* and *Grg4* (*Tle4* – Mouse Genome Informatics) are normally involved in repression of Fgf8 in the mes, it was unclear how Fgf8 becomes downregulated in dorsal r1 (Ye et al., 2001). Our study of *Gli3* mutants indicates a role for Gli3R in the initial downregulation of *Fgf8* in r1, as well as a continued requirement that extends beyond E9.0 in maintaining the dorsal restriction of *Fgf8* to the isthmus. Alternatively, Gli3 might be required to maintain dorsal-medial r1 identity, and the expansion of *Fgf8* expression is a secondary consequence of a mixed r1/isthmus identity. Interestingly, a similar interaction between Shh, Gli3 and Fgf8 exists in the developing telencephalon (Gutin et al., 2006; Kuschel et al., 2003; Ohkubo et al., 2002), suggesting that the interplay between these two signaling pathways constitutes a more general mechanism in the patterning of three-dimensional brain structures.

Regulation of cerebellum and isthmus development by Gli3R is dependent on restricting *Fgf8* to the isthmus

Based on Fgf8 loss- and gain-of-function studies, the observed ectopic expression of *Fgf8* in dorsal r1 of *Gli3* mutants could affect both tectum and cerebellum development (Zervas et al., 2005). To test this possibility, we analyzed $Gli3^{-/-}$ mutants in which one copy of *Fgf8* was removed. Strikingly, we found that whereas the isthmic-cerebellar region phenotype is partially rescued in $Gli3^{-/-};Fgf8^{+/-}$ mutants, the defects in tectal growth and IC patterning were largely not attenuated. The lack of influence of Fgf8 on mes development

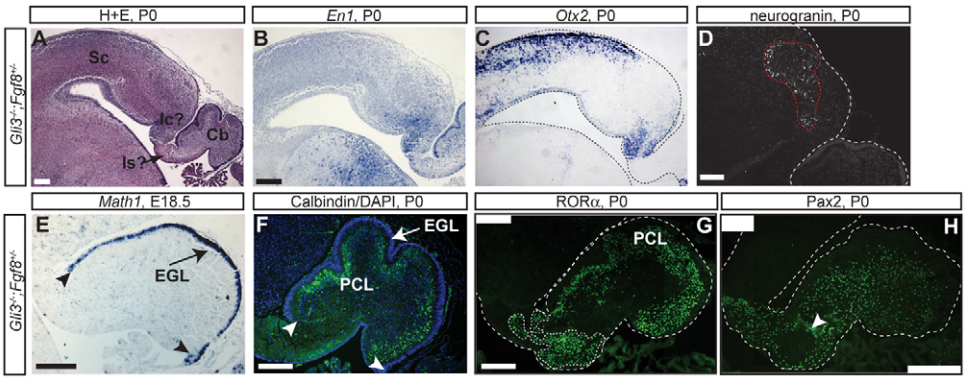

Fig. 7. Partial rescue of the *Gli3*$^{-/-}$ mutant phenotype in *Gli3*$^{-/-}$;*Fgf8*$^{+/-}$ mutants. (**A**) H+E staining on *Gli3*$^{-/-}$;*Fgf8*$^{+/-}$ mutant sagittal sections. The morphology of the Cb and Is, but not of the tectum (Sc and Ic), appears to be partially rescued in *Gli3*$^{-/-}$;*Fgf8*$^{+/-}$ mutants. (**B-D**) *En1* and *Otx2* RNA expression and immunohistochemistry for neurogranin (D, red outline) show that the Ic is not properly established in *Gli3*$^{-/-}$;*Fgf8*$^{+/-}$ mutants. (**E**,**F**) *Math1* RNA expression (E) and DAPI staining (F, blue) show that the EGL expands from the posterior Cb to the Is (arrowheads), comparable to WT. (F,**G**) Immunohistochemistry for calbindin and RORα (green) show a relatively normal PCL, but a significant number of PCs are located in clusters in the deeper Cb and Is (G, outlined). (**H**) Pax2-positive cells (green) are found in the Is, but are excluded from PC clusters (arrowhead). Scale bars: 200 μm.

is likely to be because an insufficient level of Fgf8 signaling is attained in the mes, consistent with the observation that *Spry1* is not obviously upregulated in the mes of *Gli3* mutants.

Interestingly, even though *Fgf8* expression is expanded in both *Gli3*$^{-/-}$ and *En1-Gli3* cko mutants at E10.5, the cerebellar defects are much more severe in *Gli3*$^{-/-}$ mutants. In *Gli3*$^{-/-}$ mutants, the cerebellar cytoarchitecture is severely altered and foliation is not initiated by P0. By contrast, inactivation of *Gli3* after E9.0 results in only mild cytoarchitectural defects in the cerebellum and a normal onset of foliation, but abnormal foliation pattern. Preliminary analysis of *En1-Gli3* cko mutants in which one copy of *Fgf8* had been removed found that the foliation pattern is still abnormal (S.B., unpublished). One possibility is that the foliation defects in *En1-Gli3* cko mutants are independent of ectopic Fgf8 and instead are directly caused by the loss of *Gli3*.

Attenuation of mes growth by Gli3R

One striking phenotype in the *Gli3*-null and cko mutants is the extensive overgrowth of tectal tissue. It has previously been shown that ectopic activation of the Shh pathway by misexpression of either Shh or GliA results in a pronounced overgrowth of the spinal cord, mes/r1 and postnatal cerebellum in chick and mouse (Cayuso et al.,

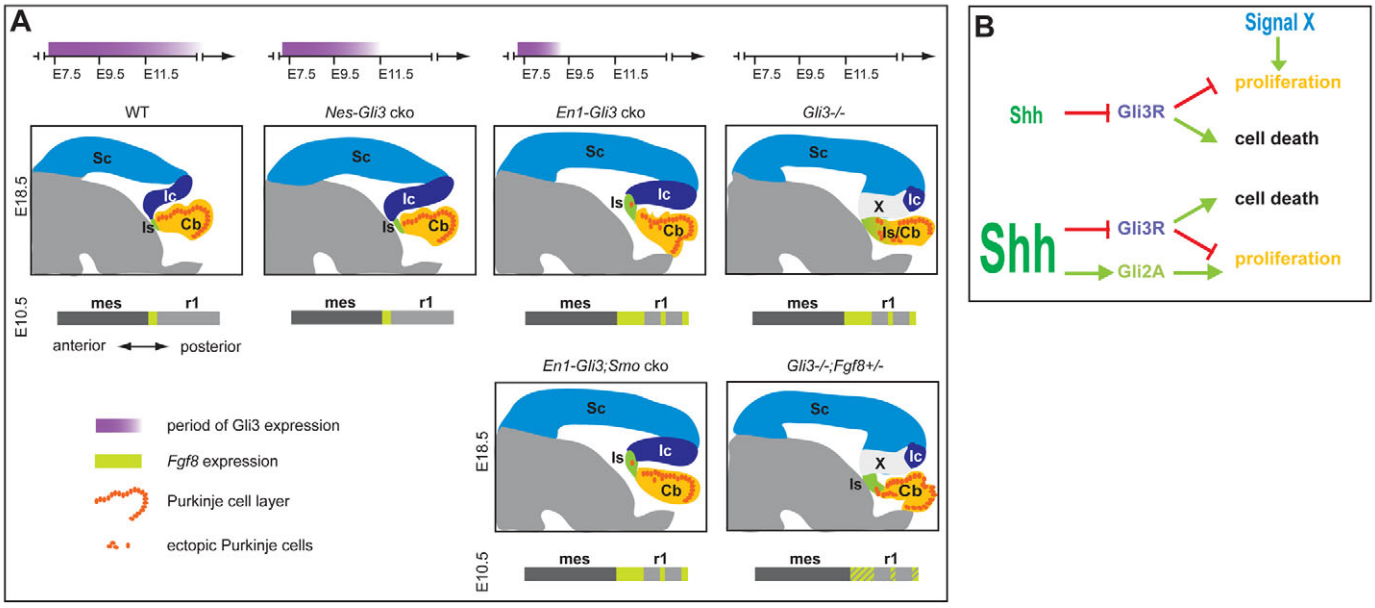

Fig. 8. The distinct temporal roles of Gli3R in regulating mouse mes/r1 development. (**A**) Time period of *Gli3* expression, prenatal tectum and cerebellum phenotype and ectopic *Fgf8* expression. Note that in *Gli3*$^{-/-}$ mutants, a domain (X) forms between the tectum and cerebellum that is not properly specified as cerebellum (Cb), isthmus (Is) or inferior colliculus (Ic). Sc, superior colliculus. See Discussion for details. (**B**) High levels of Shh (lower pathway) regulate mes/r1 growth through induction of proliferation via Gli2A and/or by inhibition of cell death through Gli3R. Low levels of Shh (upper pathway) do not induce proliferation, but modulate cell death and proliferation [induced by unknown signal (X)] through the regulation of Gli3R levels.

2006; Corrales et al., 2006; Dahmane and Ruiz-i-Altaba, 1999; Rowitch et al., 1999). The increased size of the tectum that we documented in *Gli3* and *Gli3/Smo* mutants, however, demonstrates that removing Gli3R, without an associated ectopic activation of Gli activator function, can cause increased proliferation and overgrowth. Furthermore, Gli3R is normally required beyond E11.5 to attenuate growth of the dorsal mes.

Our present results taken together with previous studies (Blaess et al., 2006; Britto et al., 2002; Ishibashi and McMahon, 2002; Corrales et al., 2006) suggest several mechanisms by which Gli transcription factors regulate tissue growth. At high levels of signaling, Shh can simply increase proliferation by upregulating GliA (primarily Gli2) such as in cerebellar granule cell precursors (Corrales et al., 2006), and/or by downregulating Gli3R such as in the ventral midbrain (Blaess et al., 2006). At low levels of Shh signaling, such as in the dorsal mes, GliA is not induced, and Shh increases overall growth only by downregulating Gli3R levels which leads to increased proliferation and cell survival (summarized in Fig. 8B). The latter reveals that other signaling pathways must stimulate proliferation of dorsal mes progenitors and a certain level of Gli3R is required only to attenuate growth.

A possible candidate to regulate proliferation in the dorsal mes is Wnt1, as it can induce overgrowth of the posterior mes (Panhuysen et al., 2004) and recent studies have provided evidence that Gli3R inhibits canonical Wnt signaling in several different tissues and cell types (Alvarez-Medina et al., 2008; Ulloa et al., 2007). However, our analysis of *Axin2* expression (a readout for canonical Wnt signaling) in the mes of *Gli3* mutants provided no evidence that *Gli3* is required in the dorsal mes to antagonize Wnt signaling. Furthermore, our preliminary analysis of $Gli3^{-/-};Wnt1^{sw/sw}$ double mutants revealed that the size of the SC is comparable to that of $Gli3^{-/-}$ mutants, although the IC (and medial cerebellum) is lost in both $Wnt1^{sw/sw}$ and $Gli3^{-/-};Wnt1^{sw/sw}$ mutants (S.B., unpublished). It is possible, however, that additional members of the Wnt family stimulate dorsal mes growth and that their action is normally attenuated by Gli3R.

In summary, we have found that the precise regulation of Gli3R levels is crucial to establish the intricate structures of the mature tectum and cerebellum. Our data provide insight into how Gli3R coordinates the function of two distinct organizer molecules in the mes/r1 by modulating their expression or downstream signaling. It will be interesting to investigate whether Gli3R plays similar complex roles in other tissues that undergo organizer-dependent three-dimensional patterning and growth.

We thank Drs F. Costantini and K. Millen for providing RNA in situ probes; the Developmental Studies Hybridoma Bank for the Nkx6.1 antibody; Frada Berenstehyn for excellent technical help; Jaden Hastings for help with sequence analysis; and Anamaria Sudarov, Charles Levine, Emilie Legue and Roy Sillitoe for critical reading of the manuscript. This work was funded by grant R01 CA128158 from NICHD. S.B. was supported by a DFG postdoctoral fellowship.

Supplementary material

Supplementary material for this article is available at http://dev.biologists.org/cgi/content/full/135/12/2093/DC1

References

Agarwala, S., Sanders, T. A. and Ragsdale, C. W. (2001). Sonic hedgehog control of size and shape in midbrain pattern formation. *Science* **291**, 2147-2150.

Alder, J., Lee, K. J., Jessell, T. M. and Hatten, M. E. (1999). Generation of cerebellar granule neurons in vivo by transplantation of BMP-treated neural progenitor cells. *Nat. Neurosci.* **2**, 535-540.

Alvarez-Medina, R., Cayuso, J., Okubo, T., Takada, S. and Marti, E. (2008). Wnt canonical pathway restricts graded Shh/Gli patterning activity through the regulation of Gli3 expression. *Development* **135**, 237-247.

Aoto, K., Nishimura, T., Eto, K. and Motoyama, J. (2002). Mouse GLI3 regulates Fgf8 expression and apoptosis in the developing neural tube, face, and limb bud. *Dev. Biol.* **251**, 320-332.

Auerbach, W., Dunmore, J. H., Fairchild-Huntress, V., Fang, Q., Auerbach, A. B., Huszar, D. and Joyner, A. L. (2000). Establishment and chimera analysis of 129/SvEv- and C57BL/6-derived mouse embryonic stem cell lines. *Biotechniques* **29**, 1024-1028, 1030, 1032.

Bai, C. B., Auerbach, W., Lee, J. S., Stephen, D. and Joyner, A. L. (2002). Gli2, but not Gli1, is required for initial Shh signaling and ectopic activation of the Shh pathway. *Development* **129**, 4753-4761.

Bai, C. B., Stephen, D. and Joyner, A. L. (2004). All mouse ventral spinal cord patterning by hedgehog is Gli dependent and involves an activator function of Gli3. *Dev. Cell* **6**, 103-115.

Bayly, R. D., Ngo, M., Aglyamova, G. V. and Agarwala, S. (2007). Regulation of ventral midbrain patterning by Hedgehog signaling. *Development* **134**, 2115-2124.

Beermann, F., Kaloulis, K., Hofmann, D., Murisier, F., Bucher, P. and Trumpp, A. (2006). Identification of evolutionarily conserved regulatory elements in the mouse Fgf8 locus. *Genesis* **44**, 1-6.

Bei, M. and Maas, R. (1998). FGFs and BMP4 induce both Msx1-independent and Msx1-dependent signaling pathways in early tooth development. *Development* **125**, 4325-4333.

Blaess, S., Corrales, J. D. and Joyner, A. L. (2006). Sonic hedgehog regulates Gli activator and repressor functions with spatial and temporal precision in the mid/hindbrain region. *Development* **133**, 1799-1809.

Britto, J., Tannahill, D. and Keynes, R. (2002). A critical role for sonic hedgehog signaling in the early expansion of the developing brain. *Nat. Neurosci.* **5**, 103-110.

Cayuso, J., Ulloa, F., Cox, B., Briscoe, J. and Marti, E. (2006). The Sonic hedgehog pathway independently controls the patterning, proliferation and survival of neuroepithelial cells by regulating Gli activity. *Development* **133**, 517-528.

Chenn, A. and Walsh, C. A. (2002). Regulation of cerebral cortical size by control of cell cycle exit in neural precursors. *Science* **297**, 365-369.

Chi, C. L., Martinez, S., Wurst, W. and Martin, G. R. (2003). The isthmic organizer signal FGF8 is required for cell survival in the prospective midbrain and cerebellum. *Development* **130**, 2633-2644.

Corrales, J. D., Rocco, G. L., Blaess, S., Guo, Q. and Joyner, A. L. (2004). Spatial pattern of sonic hedgehog signaling through Gli genes during cerebellum development. *Development* **131**, 5581-5590.

Corrales, J. D., Blaess, S., Mahoney, E. M. and Joyner, A. L. (2006). The level of sonic hedgehog signaling regulates the complexity of cerebellar foliation. *Development* **133**, 1811-1821.

Crossley, P. H. and Martin, G. R. (1995). The mouse Fgf8 gene encodes a family of polypeptides and is expressed in regions that direct outgrowth and patterning in the developing embryo. *Development* **121**, 439-451.

Dahmane, N. and Ruiz-i-Altaba, A. (1999). Sonic hedgehog regulates the growth and patterning of the cerebellum. *Development* **126**, 3089-3100.

Dai, P., Akimaru, H., Tanaka, Y., Maekawa, T., Nakafuku, M. and Ishii, S. (1999). Sonic Hedgehog-induced activation of the Gli1 promoter is mediated by GLI3. *J. Biol. Chem.* **274**, 8143-8152.

Fedtsova, N. and Turner, E. E. (2001). Signals from the ventral midline and isthmus regulate the development of Brn3.0-expressing neurons in the midbrain. *Mech. Dev.* **105**, 129-144.

Fuccillo, M., Joyner, A. L. and Fishell, G. (2006). Morphogen to mitogen: the multiple roles of hedgehog signalling in vertebrate neural development. *Nat. Rev. Neurosci.* **7**, 772-783.

Graus-Porta, D., Blaess, S., Senften, M., Littlewood-Evans, A., Damsky, C., Huang, Z., Orban, P., Klein, R., Schittny, J. C. and Muller, U. (2001). Beta1-class integrins regulate the development of laminae and folia in the cerebral and cerebellar cortex. *Neuron* **31**, 367-379.

Grove, E. A., Tole, S., Limon, J., Yip, L. and Ragsdale, C. W. (1998). The hem of the embryonic cerebral cortex is defined by the expression of multiple Wnt genes and is compromised in Gli3-deficient mice. *Development* **125**, 2315-2325.

Gutin, G., Fernandes, M., Palazzolo, L., Paek, H., Yu, K., Ornitz, D. M., McConnell, S. K. and Hebert, J. M. (2006). FGF signalling generates ventral telencephalic cells independently of SHH. *Development* **133**, 2937-2946.

Hu, M. C., Mo, R., Bhella, S., Wilson, C. W., Chuang, P. T., Hui, C. C. and Rosenblum, N. D. (2006). GLI3-dependent transcriptional repression of Gli1, Gli2 and kidney patterning genes disrupts renal morphogenesis. *Development* **133**, 569-578.

Hui, C. C. and Joyner, A. L. (1993). A mouse model of greig cephalopolysyndactyly syndrome: the extra-toesJ mutation contains an intragenic deletion of the Gli3 gene. *Nat. Genet.* **3**, 241-246.

Hui, C. C., Slusarski, D., Platt, K. A., Holmgren, R. and Joyner, A. L. (1994). Expression of three mouse homologs of the Drosophila segment polarity gene cubitus interruptus, Gli, Gli-2, and Gli-3, in ectoderm- and mesoderm-derived tissues suggests multiple roles during postimplantation development. *Dev. Biol.* **162**, 402-413.

Ishibashi, M. and McMahon, A. P. (2002). A sonic hedgehog-dependent signaling relay regulates growth of diencephalic and mesencephalic primordia in the early mouse embryo. *Development* **129**, 4807-4819.
Jacob, J. and Briscoe, J. (2003). Gli proteins and the control of spinal-cord patterning. *EMBO Rep.* **4**, 761-765.
Jho, E. H., Zhang, T., Domon, C., Joo, C. K., Freund, J. N. and Costantini, F. (2002). Wnt/beta-catenin/Tcf signaling induces the transcription of Axin2, a negative regulator of the signaling pathway. *Mol. Cell. Biol.* **22**, 1172-1183.
Kimmel, R. A., Turnbull, D. H., Blanquet, V., Wurst, W., Loomis, C. A. and Joyner, A. L. (2000). Two lineage boundaries coordinate vertebrate apical ectodermal ridge formation. *Genes Dev.* **14**, 1377-1389.
Kuschel, S., Ruther, U. and Theil, T. (2003). A disrupted balance between Bmp/Wnt and Fgf signaling underlies the ventralization of the Gli3 mutant telencephalon. *Dev. Biol.* **260**, 484-495.
Li, J. Y., Lao, Z. and Joyner, A. L. (2002). Changing requirements for Gbx2 in development of the cerebellum and maintenance of the mid/hindbrain organizer. *Neuron* **36**, 31-43.
Liu, A., Li, J. Y., Bromleigh, C., Lao, Z., Niswander, L. A. and Joyner, A. L. (2003). FGF17b and FGF18 have different midbrain regulatory properties from FGF8b or activated FGF receptors. *Development* **130**, 6175-6185.
Maricich, S. M. and Herrup, K. (1999). Pax-2 expression defines a subset of GABAergic interneurons and their precursors in the developing murine cerebellum. *J. Neurobiol.* **41**, 281-294.
Marigo, V., Johnson, R. L., Vortkamp, A. and Tabin, C. J. (1996). Sonic hedgehog differentially regulates expression of GLI and GLI3 during limb development. *Dev. Biol.* **180**, 273-283.
Matise, M., Auerbach, W. and Joyner, A. L. (2000). Production of targeted embryonic stem cell clones. In *Gene Targeting: A Practical Approach* (ed. A. L. Joyner). New York: Oxford University Press.
Maynard, T. M., Jain, M. D., Balmer, C. W. and LaMantia, A. S. (2002). High-resolution mapping of the Gli3 mutation extra-toes reveals a 51.5-kb deletion. *Mamm. Genome* **13**, 58-61.
Ohkubo, Y., Chiang, C. and Rubenstein, J. L. (2002). Coordinate regulation and synergistic actions of BMP4, SHH and FGF8 in the rostral prosencephalon regulate morphogenesis of the telencephalic and optic vesicles. *Neuroscience* **111**, 1-17.
Panhuysen, M., Vogt Weisenhorn, D. M., Blanquet, V., Brodski, C., Heinzmann, U., Beisker, W. and Wurst, W. (2004). Effects of Wnt1 signaling on proliferation in the developing mid-/hindbrain region. *Mol. Cell. Neurosci.* **26**, 101-111.
Papaioannou, V. and Johnson, R. (2000). Production of chimeras by blastocyst and morula injection of targeted ES-cells. In *Gene Targeting: A Practical Approach* (ed. A. L. Joyner), pp. 133-175. Oxford: Oxford University Press.
Pedersen, I. L., Klinck, R., Hecksher-Sorensen, J., Zahn, S., Madsen, O. D., Serup, P. and Jorgensen, M. C. (2006). Generation and characterization of monoclonal antibodies against the transcription factor Nkx6.1. *J. Histochem. Cytochem.* **54**, 567-574.
Rodriguez, C. I., Buchholz, F., Galloway, J., Sequerra, R., Kasper, J., Ayala, R., Stewart, A. F. and Dymecki, S. M. (2000). High-efficiency deleter mice show that FLPe is an alternative to Cre-loxP. *Nat. Genet.* **25**, 139-140.
Rowitch, D. H., St.-Jacques, B., Lee, S. M. K., Flax, J. D., Snyder, E. Y. and McMahon, A. P. (1999). Sonic hedgehog regulates proliferation and inhibits differentiation of CNS precursor cells. *J. Neurosci.* **19**, 8954-8965.
Sgaier, S. K., Lao, Z., Villanueva, M. P., Berenshteyn, F., Stephen, D., Turnbull, R. K. and Joyner, A. L. (2007). Genetic subdivision of the tectum and cerebellum into functionally related regions based on differential sensitivity to engrailed proteins. *Development* **134**, 2325-2335.
Theil, T., Aydin, S., Koch, S., Grotewold, L. and Ruther, U. (2002). Wnt and Bmp signalling cooperatively regulate graded Emx2 expression in the dorsal telencephalon. *Development* **129**, 3045-3054.
Tronche, F., Kellendonk, C., Kretz, O., Gass, P., Anlag, K., Orban, P. C., Bock, R., Klein, R. and Schutz, G. (1999). Disruption of the glucocorticoid receptor gene in the nervous system results in reduced anxiety. *Nat. Genet.* **23**, 99-103.
Ulloa, F., Itasaki, N. and Briscoe, J. (2007). Inhibitory Gli3 activity negatively regulates Wnt/beta-catenin signaling. *Curr. Biol.* **17**, 545-550.
Vokes, S. A., Ji, H., McCuine, S., Tenzen, T., Giles, S., Zhong, S., Longabaugh, W. J., Davidson, E. H., Wong, W. H. and McMahon, A. P. (2007). Genomic characterization of Gli-activator targets in sonic hedgehog-mediated neural patterning. *Development* **134**, 1977-1989.
Wang, B., Fallon, J. F. and Beachy, P. A. (2000). Hedgehog-regulated processing of Gli3 produces an anterior/posterior repressor gradient in the developing vertebrate limb. *Cell* **100**, 423-434.
Wang, C., Ruther, U. and Wang, B. (2007). The Shh-independent activator function of the full-length Gli3 protein and its role in vertebrate limb digit patterning. *Dev. Biol.* **305**, 460-469.
Wurst, W. and Bally-Cuif, L. (2001). Neural plate patterning: upstream and downstream of the isthmic organizer. *Nat. Rev. Neurosci.* **2**, 99-108.
Xu, J., Liu, Z. and Ornitz, D. M. (2000). Temporal and spatial gradients of Fgf8 and Fgf17 regulate proliferation and differentiation of midline cerebellar structures. *Development* **127**, 1833-1843.
Ye, W., Bouchard, M., Stone, D., Liu, X., Vella, F., Lee, J., Nakamura, H., Ang, S. L., Busslinger, M. and Rosenthal, A. (2001). Distinct regulators control the expression of the mid-hindbrain organizer signal FGF8. *Nat. Neurosci.* **4**, 1175-1181.
Zervas, M., Blaess, S. and Joyner, A. L. (2005). Classical embryological studies and modern genetic analysis of midbrain and cerebellum development. *Curr. Top. Dev. Biol.* **69**, 101-138.